# Genome-wide associations of schizophrenia studied with computer simulation

Samuel A Neymotin[1]

Mohamed A Sherif[1,3]

Jeeyune Q Jung[1]

Joseph J Kabariti[1]

William W Lytton[1,2]

[1] Dept. Physiology & Pharmacology, SUNY Downstate, Brooklyn, NY

[2] Dept. Neurology, Kings County Hospital Center, Brooklyn, NY

[3] Dept. Psychiatry, Yale University and VA Healthcare, New Haven, CT

August 8, 2016

# Overview

Schizophrenia is a mysterious disease, striking directly at attributes of thought and personality that make one a person. Although a brain disease, it is handled by psychiatry rather than neurology, since long mistakenly thought to be a problem entirely of nurture, purely a disease of mind, rather than a brain disease. The hippocampus and associated areas are part of a complex of brain areas involved in schizophrenic pathology, but these medial telencephalic areas are of particular interest. In this chapter, we will follow a multiscale modeling approach focused on area CA3 of hippocampus. The scales to be considered start at the molecular scale of receptor physiology, proceed through cellular and network dynamics, then up to the scale of information transmission – taken as a proxy for cognitive function. As part of the evaluation of network dynamics, we consider the role of oscillations, hypothesized to provide a glue that provides the neural coordination that underlies cognitive coordination (Bressler and Kelso, 2001). Oscillations within and between different brain areas are thought to synchronize the firing of networks that are functionally related.

## Schizophrenia: clinical pathways of disorder

A recent genome-wide association study (GWAS) demonstrated 108 association loci that are associated with development of schizophrenia (Schizophrenia Working Group, 2014). These are just the sites that can be implicated using the statistical power conferred by current data. It is expected that many more sites will be uncovered as new studies use larger numbers of cases and controls. The number of likely associated loci is uncertain, but one estimate suggests it may be in the thousands (International Schizophrenia Consortium *et al.*, 2009). For any given patient, only a small subset of these locations will show mutations. The *clinical pathway hypothesis* for polygenic diseases predicts that the various sites of damage associated with a given disease reflect sets of mutationally damaged genes that together produce the disease (we will use the term *clinical pathway* so as to distinguish it from the traditional definition of a *pathway* as a biochemical sequence) (Sullivan, 2012). What is a clinical pathway? This term remains weakly defined, and will differ between diseases, and even within a single disease. For example, multiple clinical pathways

in schizophrenia may well involve **1.** developmental sequences, **2.** intracellular cascade sequences such as second-messenger cascades in neurons, **3.** genetic activation sequences or RNA transcriptional control sequences, **4.** immunological and scavenging pathways (*e.g.,* synapse and cell elimination in schizophrenia(Sullivan, 2012)) **5.** pathways of dynamical physiological interactions that together provide physiological activity.

Schizophrenia is triggered by insults and anomalies that act at various times of life. Susceptibility at each of these stages of pathological influence would be expected to be associated with a different clinical pathway, or set of clinical pathways. One clinical pathway would confer susceptibility to the peri-natal insult that is believed to predispose to the disease. Subsequently, there is a likelihood of a clinical pathway involving synaptic pruning in late adolescence (Sekar et al., 2016). This may be the same or different from a clinical pathway that confers susceptibility in response to external stress, an important factor in the onset of clinical disease (Tost and Meyer-Lindenberg, 2012). Finally, there will be one or more clinical pathways that produce the various signs and symptoms of schizophrenia – cognitive disorder, positive symptoms such as hallucinations, and negative symptoms of social withdrawal.

Given this complexity, it is expected that multiple pathway "hits," with various hits within each involved pathway, determines the clusters of clinical manifestations that make it difficult to clearly define schizophrenia or to define clinical subtypes (Tandon et al., 2013). The welter of schizophrenia definitions, and the mix of symptoms, has led the U.S. National Institute of Mental Health to move away from symptom-based disease definition in favor of future biomarker-based diagnosis (Insel et al., 2010). In this context, one notes the genetic overlap with other disorders that feature particular symptoms of schizophrenia: bipolar disorder in which one may have hallucinations, and autism whose characteristic feature is social withdrawal (Sullivan, 2012). At some schizophrenia-associated loci, a more damaging mutation will produce one of these other disorders, rather that a more severe form of schizophrenia.

. In this chapter, we discuss our explorations of alterations in theta and gamma activity in hippocampal area CA3, using multiscale modeling to show how changes in ion channels at molecular scale will alter network activity. We then show how anomalies in brain waves can be correlated with explicit

alterations in information flow (measured using information theory), and thereby could help explain alterations in cognitive function.

## $I_{\mathrm{h}}$ and NMDA as clinical pathway partners

We focus here on two identified genomic/proteomic factors that we have studied through physiological simulation: $I_{\mathrm{h}}$ channels and NMDA receptors (Neymotin et al., 2011b; Neymotin et al., 2016; Neymotin et al., 2013). We propose that these mutations will be part of the same clinical pathway involved in generating oscillations (a potential biomarker), and in producing the cognitive dysfunction hypothesized to be an underlying disorder in schizophrenia (Franck et al., 2013). $I_{\mathrm{h}}$ current is mediated by hyperpolarization-activated cyclic nucleotide-gated (HCN) channels. A putative mutation in the HCN1 gene (5p21) is near one of the 108 loci implicated in schizophrenia (Schizophrenia Working Group, 2014). The other implicated mutation that we study here is in the GRIN2A gene (glutamate ionotropic NMDA-type receptor subunit 2A on 16p13), a subunit that forms part of the ionotropic NMDA-type glutamatergic receptor (NMDAR). Changes in either the NMDAR synaptic current or in $I_{\mathrm{h}}$ will alter cortical oscillations. Of course, additional factors will also be expected to be involved in this clinical pathway, altering cortical oscillations. For example, basket cell number is reduced in schizophrenia (Lewis et al., 2012). These cells play an important role in generating fast oscillations through PING (pyramidal-interneuron network gamma) and ING (interneuron network gamma) mechanisms (Cobb et al., 1995; Lytton and Sejnowski, 1991a).

A recent set of observations indicates that patients diagnosed with schizophrenia have increased spontaneous and driven gamma (30-80 Hz) compared to controls (Hirano et al., 2015). Other studies have shown differences in gamma activation between patients and controls performing complicated recognition tasks (Uhlhaas et al., 2008; Uhlhaas and Singer, 2010). These changes in gamma are similar to what is seen in animal models of schizophrenia (Lazarewicz et al., 2010; Lee et al., 2014). Animal models also show a reduction in theta power (6-10 Hz with different ranges by species). We focused on these two physiological markers, using alterations in gamma or in theta-gamma balance as an indicator of pathology in our simulations. Network oscillation anomalies are also implicated in the genesis and expression of many

other neurological and psychiatric disorders, including the epilepsies (Lytton, 2008) and mild cognitive impairment (Moretti et al., 2013; de Haan et al., 2012).

The **HCN** ion channel, providing current $I_{\mathrm{h}}$, is a voltage-gated channel involved in maintaining resting potential, augmenting sub-threshold resonance, and providing depolarization with activation (Accili et al., 2002; Chen et al., 2001; Santoro and Baram, 2003; Zemankovics et al., 2010; Dyhrfjeld-Johnsen et al., 2008; Dyhrfjeld-Johnsen et al., 2009; Poolos et al., 2002). HCN has 4 defined isoforms (HCN1–HCN4); HCN1 and HCN2 are the dominant forms in neurons. HCN1 is implicated in schizophrenia. Inhomogeneous isoform distributions of the HCN channel leads to differential expression and modulation of $I_{\mathrm{h}}$ in different cell types (Accili et al., 2002; Aponte et al., 2006; Bender et al., 2001; Santoro and Baram, 2003). Neurotransmitters from different brain areas and local neuromodulators provide multiple pathways for regulating $I_{\mathrm{h}}$ (Hagiwara and Irisawa, 1989). Multiple functions, multiple types, and multiple routes for modulation make HCN a complex control point in the circuit. HCN channels are unusual in terms of their behavior compared to other voltage- and ligand-sensitive membrane channels. The HCN-associated current is called an *anomalous rectifier* because activated by neuronal membrane hyperpolarization (hence $I_{\mathrm{h}}$), rather than by the depolarization that is typical for most voltage-gated ion channels. $I_{\mathrm{h}}$ is also unusual in having an intermediate reversal potential (-30 to -40 mV).

The focus of much literature on **NMDAR** has been on the role that it plays in plasticity, specifically on long-term potentiation. In that context, NMDAR serves an adjunctive role by signaling, via calcium levels, an activity level which is then translated into altered synaptic strength (Lisman and Raghavachari, 2006; Serulle et al., 2007). A separate, but likely related, aspect of NMDAs role is as a synaptic receptor and ionotropic channel that complements AMPA in excitatory activation of a postsynaptic cell (Chover et al., 2001; Hasselmo and Bower, 1992; Hasselmo, 2005). NMDAR is voltage-dependent via a $Mg^{+2}$ blockade that is relieved by postsynaptic depolarization. It shows permeability to both $Ca^{2+}$ and $Na^{+}$ so that activation provides a local depolarization, as well as $Ca^{2+}$ signaling of postsynaptic cascades. These direct ionotropic effects provide a postsynaptic activation that is complementary to the more rapid, earlier, and less prolonged excitatory postsynaptic potentials due to AMPA. This complementarity can be viewed as

dynamically providing the network with a second matrix of connectivity (Chover et al., 2001). Prior to the evidence from GWAS, the psychotomimetic effects of NMDA blockade with drugs such as phencyclidine (PCP) and ketamine had already suggested that NMDARs might play an important role in schizophrenia and other psychotic disorders.

## The model: cells and synapses

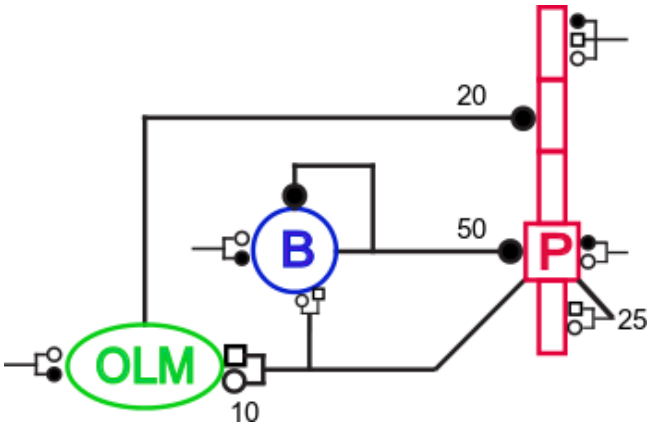


Figure 1: **Schematic representation of the network.** Each symbol represents a population: 800 pyramidal cells (red, P, PYR), 200 basket cells (blue, B, BAS), 200 oriens lacunosum-moleculare (green, OLM) cells. Convergence values (number of inputs for an individual synapse) are shown near synapses: $GABA_A$ receptors (filled circles), AMPA receptors (open circles), NMDA receptors (open squares). External stimulation from other areas was modeled by synaptic bombardment (synapses with truncated lines).

The network presented was previously used in Neymotin et al. (2011b) (ModelDB #139421) and Neymotin et al. (2013) (ModelDB #151282). Most of the results presented previously appeared, in slightly different form, in those two papers. Briefly, the network consisted of 800 5-compartment pyramidal cells, 200 one-compartment basket interneurons, and 200 one-compartment oriens lacunosum-moleculare (OLM) interneurons (Fig. 1). Current injections (pyramidal cells: 50 pA; OLM cells -25 pA) were added to get baseline activity. Additional background activity to provide ongoing synaptic excitatory and inhibitory inputs followed a Poisson process and was sent to somata of all cells and dendrites of pyramidal cells. Periodic inhibition from medial septum (MS) paced the interneurons, modeling the function of the MS as a pacemaker (Hangya et al., 2009; Stewart and Fox, 1990).

All cells contained leak current, transient sodium current $I_{Na}$, and delayed rectifier current $I_{K-DR}$, to allow for action potential generation. Additionally, pyramidal cells contained in $I_{\mathrm{A}}$ (A current) and $I_{\mathrm{h}}$ in all compartments. The OLM cells had a simple calcium-activated potassium current $I_{KCa}$ to allow long lasting inactivation after bursting, high-threshold calcium current $I_L$ to augment bursting and activate $I_{KCa}$ and intracellular $Ca^{2+}$-decay dynamics. Currents were based on prior published models (Stacey et al., 2009; Tort et al., 2007; Traub, 1982).

There were a total of 152,000 synapses. Pyramidal cell projections provided mixed AMPA and NMDA response. Basket cells synapsed on the soma of both pyramidal cells and other basket cells via $GABA_A$ receptors. OLM cells connected to distal dendrites of pyramidal cells via $GABA_A$ receptors. AMPA and NMDA receptors had reversal potentials of 0 mV, while $GABA_A$ receptors had reversal potentials of -80 mV.

Connections in the network were set up based on fixed convergences (Fig. 1). However, connectivity was random and specific divergence could therefore vary. All synaptic delays between cells were 2 ms, to simulate axonal propagation and neurotransmitter diffusion and binding, which were not explicitly modeled. Synaptic parameters were based on the literature where available, as well as on previous models (Tort et al., 2007; White et al., 2000). Parameters were tuned to reproduce theta (3-12 Hz), gamma (30-100 Hz), and theta-modulated gamma oscillations with sparse firing of pyramidal cells. The medial septum input to interneurons was simulated as 150 ms-interval synaptic conductances with rise time of 20 ms, offset time of 40 ms, and reversal potential of -80 mV.

Synapses were modeled by a standard NEURON double-exponential mechanism with parameters based on Tort et al. (2007). Magnesium block in NMDA receptors used the experimental scaling factor $1/(1 + 0.28 \cdot Mg \cdot e^{-0.062 \cdot V})$; $Mg = 1mM$ (Jahr and Stevens, 1990b). At -75 mV, AMPA response peak amplitude was 1.15 mV and NMDA response peak amplitude was 0.1 mV, whereas for -61 mV they were 1.75 mV and 0.65 mV, respectively.

## The model: network and oscillations

The network consisted of 800 five-compartment pyramidal (PYR) cells, 200 one-compartment basket (BAS) cells, and 200 one-compartment oriens lacunosum-moleculare (OLM) cells with an input from medial septum (MS; Fig. 1). The model contained 152,000 synapses, with baseline activity maintained by providing background white-noise external inputs. Basket cells synapsed on somata of both pyramidal and other basket cells. OLM cells synapsed on pyramidal cell apical dendrites. Connectivity was determined by connection densities so that specific connectivity in a given network was random. Parameters were based on the literature where available, as well as on previous computer models (Cutsuridis et al., 2010; Neymotin et al., 2011b; Tort et al., 2007; Wang, 2002; Wang and Buzsaki, 1996; White et al., 2000).

Oscillation were generated through interactions among inhibitory cells (ING), and between inhibitory cells and pyramidal cells (PING; Börgers and Kopell, 2003). The basic simulation produces theta and gamma activity (Fig. 2), measured from an LFP (top) generated from the pyramidal cells (spikes in red in raster plot at bottom). The interplay among the BAS cells produced robust ING (Buzsáki and Wang, 2012; Lytton and Sejnowski, 1991b; White et al., 2000), visualizable in the raster by noting the strong rapid synchrony among the BAS cells in green (see also Fig. 3 from Neymotin et al., 2013). Theta oscillation was augmented by oscillatory driving from the medial septum via the OLM (blue) and basket cells (green). Theta was still present in the absence of medial septum drive (Neymotin et al., 2011b).

## HCN alterations affect oscillations

Through its non-zero conductance and a relatively depolarized reversal potential ($E_h$ of -40 to -30), $I_{\mathrm{h}}$ contributes to neuronal resting membrane potential (RMP). Because of this, increase in $I_{\mathrm{h}}$ produced depolarization, leading to increased cell firing. Depolarization also increased the driving force for inhibition, and decreased the driving force for excitation. Paradoxically however, EPSP strength *increased* with increasing $I_{\mathrm{h}}$ due to a boosting effect through partial activation of sodium currents.

Control of $I_{\mathrm{h}}$ by the second messenger cAMP could permit $I_{\mathrm{h}}$ to function as a control point for

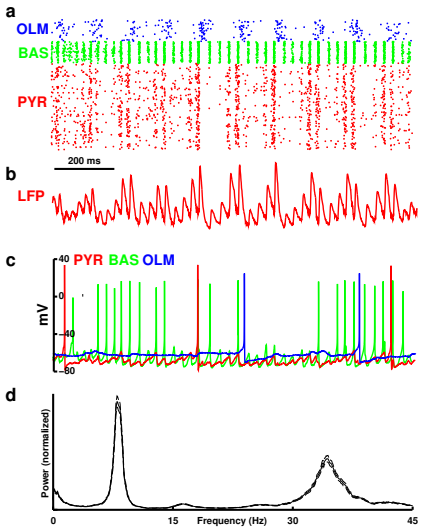


Figure 2: **Network generates theta and gamma activity.** Raster plot (bottom) shows firing times of individual cells – note the strong gamma in the green BAS cells ($\sim$ 8 cycles in 200 ms) and theta from the blue OLM cells ($\sim$ 2 cycles in 200 ms). Spectrum from local field potential (LFP, red at top) generated by PYR cells. Adapted from Neymotin et al. (2013).

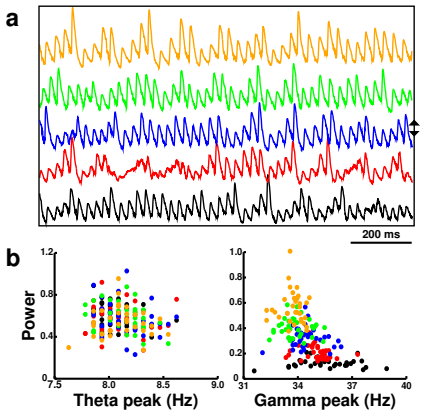


Figure 3: **Gamma power increases with $I_{\mathrm{h}}$ increase in basket (BAS) cells.** (**a**) Local field potentials (LFPs) from simulations show fast frequency power increasing with increasing BAS $I_{\mathrm{h}}$. Center shows scatter plots of theta and gamma peak frequency and power (arbitrary units) – each point from a single simulation with different random activation and wiring. Bottom shows the average power spectrum across simulations bounded by standard error of the mean (SEM). n=180 simulations; Adapted from Neymotin et al. (2013).

hippocampal oscillations. Differential activation of cAMP in different cell populations would then allow $I_h$ to have different effects depending on this modulatory activation pattern. We hypothesized that $I_h$ control on different populations would produce specific gamma or theta frequency shifts and changes in power. We looked first at effects on the BAS cells, which we predicted would give strong gamma control, since BAS activity is associated with production of gamma through both ING and PING. The simulations confirmed this effect on gamma and showed inconsistent effects on theta with different randomized networks (Fig. 3; networks are randomized with different white-noise drive and different specific wiring). With increased $I_h$ the amplitude of gamma increased (Fig. 3, top: green, orange LFPs) With decreased $I_h$, gamma amplitude was reduced (red, black LFPs). The scatter plots at center of Fig. 3 demonstrate the variability in network dynamics effects due to different random seeds. The average power spectra (Fig. 3, bottom) demonstrated the overall effect on gamma. Increased gamma with increased $I_h$ can be explained as a consequence of the increased IPSP amplitude which will tend to augment ING effects particularly, producing greater cooperativity among the BAS cells (Brody, 1999). These increased IPSPs also increased the gamma period.

Alteration of $I_h$ in OLM did not produce regular-tending effects (Fig. 4 top). Change of OLM $I_h$ in either direction tended to abolish theta – note near-zero values of theta power for $2\times$ (orange) and $0\times$ (black) at upper left. Reduced OLM $I_h$ gave extremely high gamma – $0\times$ (black) and $0.5\times$ (red) at upper right (note maximum y-axis value here). $I_h$ increase in PYR produced augmentation of theta power with a slight shift to higher frequency and little change in gamma (Fig. 4 bottom). This effect was mediated by increased PYR firing driving OLM firing. From Fig. 3 and Fig. 4, we see that BAS $I_h$ could be a control point for gamma, while PYR $I_h$ could function as a control point for theta modulation. Manipulating both PYR and BAS $I_h$ together produced augmentation of both theta and gamma power in tandem (Fig. 5). This was associated with an increase in theta frequency with a decrease in gamma frequency. Alteration of $I_h$ at all 3 sites (PYR, BAS, OLM) gave a pattern of change similar to that of OLM alone (not shown).

Pyramidal cell $I_h$ control of theta with basket cell $I_h$ control of gamma suggested that simultaneous control could be achieved through comodulation of $I_h$ in both of these cell types. This could occur either through similar control mechanisms, or through more complex modulation utilizing different sec-

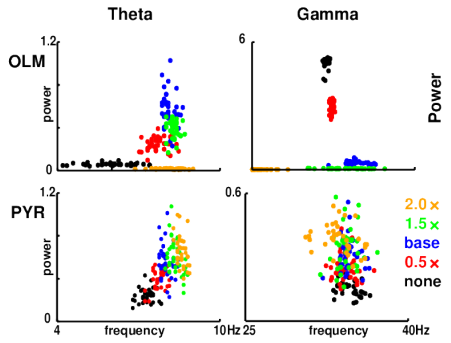


Figure 4: **Changes in theta and gamma power and frequency with alteration in OLM and PYR $I_h$.** Alterations in OLM in either direction tended to wipe out theta. Increased OLM $I_h$ also reduced gamma while decreases produced a high gamma state (note y-axis up to 6 in upper right panel). Increased PYR $I_h$ produced relatively isolated effect on theta – increasing theta power and frequency with little effect on gamma. Adapted from Neymotin et al. (2013).

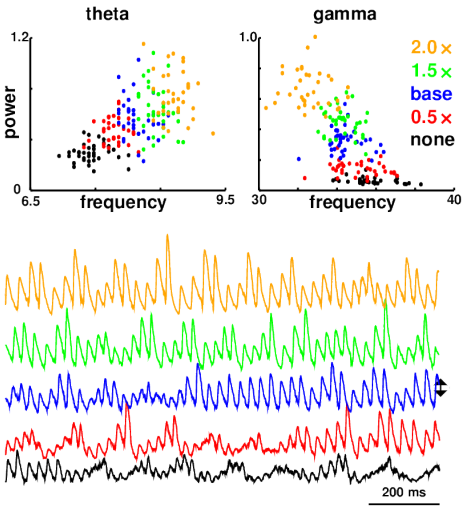


Figure 5: **Changes in theta and gamma power and frequency with simultaneous alteration in PYR and BAS $I_h$.** Augmentation at these two sites increased power in both frequency bands while increasing theta and decreasing gamma frequency.

ond messengers, different isoform second-messenger sensitivity, or neuromodulators with differing downstream effects. Cyclic adenosine monophosphate (cAMP) selectively modulates HCN2 (Wahl-Schott and Biel, 2009; Zong et al., 2012), and p38 mitogen-activated protein kinase (MAP kinase) modulates HCN1 (Poolos et al., 2006). We note here that these types of complex comodulation control mechanisms would provide many points of vulnerability along a clinical pathway, points that could be detected in the clinical population via GWAS.

Simultaneous increase of $I_{\mathrm{h}}$ at both PYR and BAS locations produced power increases in both theta and gamma (Fig. 5). Power increases and frequency shifts seen with co-modulation were similar to those produced by modulation of each independently – compare with Fig. 4 for effects on theta (lower left) and Fig. 3 for effects on gamma (arrow in Fig. 3). Relatively little cross interference was seen, not surprising in that each locus of control showed such specific effects on one frequency band, with little effect on the other. This independence was confirmed by independently altering PYR and BAS $I_{\mathrm{h}}$ (Fig. 6). There was practically no influence of BAS $I_{\mathrm{h}}$ on theta (left panel): power gradually increased with increased PYR $I_{\mathrm{h}}$ along $y$ direction with almost no alteration with changed BAS $I_{\mathrm{h}}$ (x-axis). There was however some influence of PYR $I_{\mathrm{h}}$ on gamma (center panel): high gamma required PYR $I_{\mathrm{h}}$ at or above baseline. Some effect here is expected because PYR contributes to gamma via the PING mechanism as well as by modulation of gamma by theta. This modulation of gamma by theta was measured using cross-frequency coherence (CFC; right panel): high modulation of gamma was seen with the high theta associated with high PYR $I_{\mathrm{h}}$. The influence of BAS $I_{\mathrm{h}}$ on CFC was more subtle, with the strongest modulation seen at relatively low values of BAS $I_{\mathrm{h}}$. With high values of BAS $I_{\mathrm{h}}$, the powerful gamma is high at all times and is unmodulated. Modulation of spiking by gamma and of gamma by theta has been suggested as a mechanism of item separation for short-term memory (Lisman and Idiart, 1995).

## GRIN2A effects on NMDA

GRIN2A encodes the NR2A subunit of the NMDA receptor. A mutation in this subunit could potentially alter one or more attributes of this synaptic channel, including conductance, $Mg^{+2}$ responsivity and $Zn^{+2}$

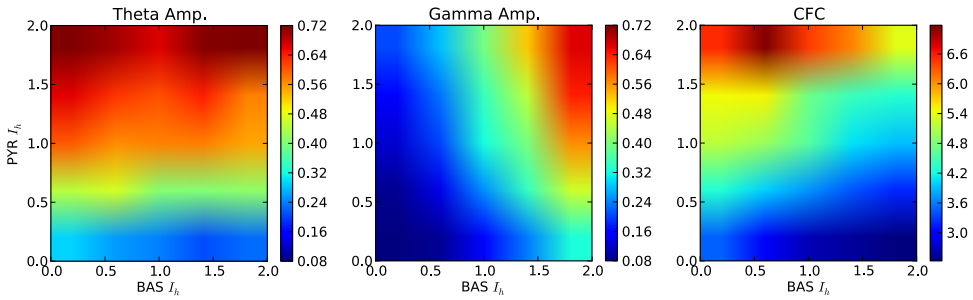


Figure 6: Changes in theta and gamma power (z-axis color code) as function of of BAS $I_{\mathrm{h}}$ augmentation (x-axis; 0× - 2× baseline values as before) and PYR $I_{\mathrm{h}}$ augmentation (y-axis; 0× - 2× baseline). Third panel shows strength of influence of theta on gamma at different values using cross-frequency coherence (CFC).

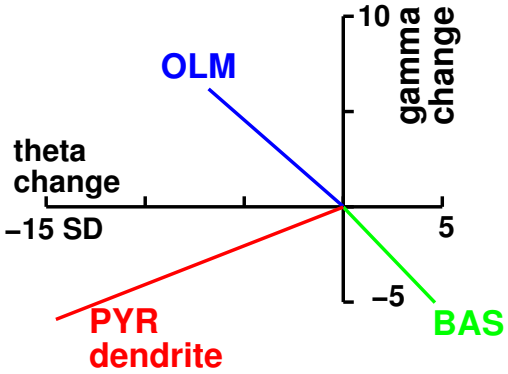


Figure 7: Changes in theta and gamma power with NMDA conductance reduction at 3 locations. OLM NMDA block increases gamma and decreases theta. PYR dendrite NMDA block produces decrease in both bands. BAS NMDA block produces reduction in gamma and increase in theta. Axes are in units of standard deviation from the mean compared to control based on 25 different simulations with different seeds. Adapted from Fig 6 of Neymotin et al. (2011b).

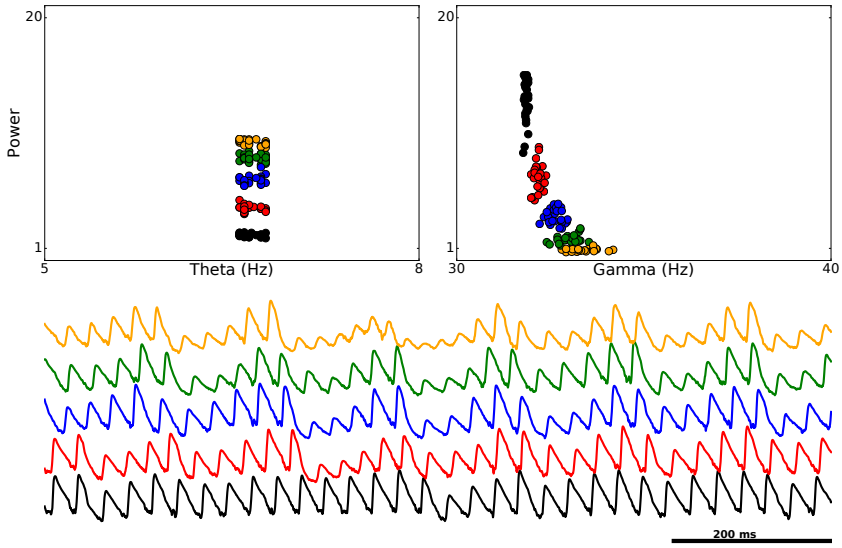


Figure 8: Shift in theta and gamma power as a function of OLM NMDAR decreased conduction from orange (high conductance, wild type) to lower conductance values in sequence: green, blue, red, black. Decreased conductance here leads to greater gamma. Note that $y$ scale measure (power) in these panels is $\sim 10\times$ prior figures measure due to use of a different LFP algorithm.

sensitivity (Cull-Candy et al., 2001). For these simulations, we assumed that the mutation would reduce NMDA conductance, and examined how decreased NMDA conductance would change network properties. As shown in Fig. 1, NMDARs are located at each of the 3 cell locations in the circuit (squares). Reducing NMDA conductance at each location produces different effects on theta and gamma waves: $\downarrow\theta\downarrow\gamma$ at PYR; $\uparrow\theta\downarrow\gamma$ at BAS; $\downarrow\theta\uparrow\gamma$ at OLM locations (Fig. 7). Combinations of block at 2 or more locations generally produced the $\downarrow\theta\downarrow\gamma$ pattern of PYR blockage (Neymotin et al., 2011b). As noted above, both animal-model and human studies of schizophrenia show gamma increase, and animal models also show theta decrease. We therefore predict that schizophrenia-associated mutations in GRIN2A would primarily reduce the conductance for OLM NMDAR, producing this increased gamma and decreased theta. This further predicts that one or both of the OLM NMDAR NR2 wildtype isoforms would be NR2A. This could be tested *in vitro* using the characteristic effects of TPEN (a zinc chelator) on NR2A-containing NMDARs (Cull-Candy et al., 2001). An alternative hypothesis would be that gamma increase could be produced by a GRIN2A-based NR2A conductance *increase* at one of the other two sites, BAS or PYR.

Gradual reduction of OLM NMDA conductance produced gradual augmentation of gamma with

decrement in theta power, associated with a slight shift of gamma peak frequency (Fig. 8). Note that the increase in gamma seen here occurs with *decreased* NMDAR conductance, opposed to the direction of effect of $I_{\mathrm{h}}$, where increased gamma was seen with increased $I_{\mathrm{h}}$ conductance in BAS (Fig. 3). With OLM NMDAR conductance decrease we have a single location which alters both gamma and theta in tandem – increasing gamma and reducing theta. By contrast, when changing $I_{\mathrm{h}}$ we found that one location, BAS $I_{\mathrm{h}}$, primarily controlled gamma, while another locations, PYR $I_{\mathrm{h}}$, controlled theta (Fig. 6).

## Information flow-through

In addition to assessing the effects on frequency, we evaluated how alterations in dynamics would change the ability of our CA3 network to accurately convey signals. This is important because it starts to make the connection between dynamics – the study of how neurons and networks are active over time through spiking and oscillations – and *information*, in the Shannon information theoretic sense (Shannon and Weaver, 1949). Shannon information theory is concerned with abstract symbols and signals rather than with the meaning, if any, of a symbol or signal. However, in the quest to examine correlation and causality between neurodynamics and cognitive representations, information theory does represent an important first step. This connection is particularly relevant to schizophrenia, whose manifestations include alterations in thought processing, changes in cognition and sensory processing, and difficulties in distinguishing external stimuli from internal activations – hallucinations.

It is currently believed that the pathology of schizophrenia involves a *cognitive core* that underlies the more obvious positive symptoms (*e.g.,* hallucinations and delusions) and negative symptoms (*e.g.,* social withdrawal) (Silverstein et al., 2006; Uhlhaas et al., 2006b; Uhlhaas et al., 2006c). The difficulty in cognitive coordination associated with schizophrenia can be shown by assessing the patient's ability to identify a complex object, a gestalt. Gestalt perception requires *binding* many individual aspects of a scene, pulling them together to see an object – for example the camouflaged animal in Fig. 9 (Uhlhaas and Silverstein, 2005). Gestalt perception requires coordination of activity across multiple areas of cortex, all the more so when a perception is multisensory rather than just visual. This *neural coordination*

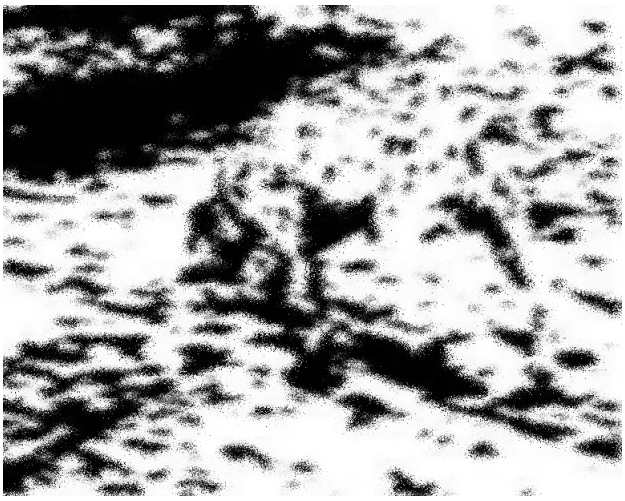

Figure 9: There is a dog hidden in this picture. If you're having difficulty finding it search internet images "gestalt dog speckle" for a guided tour of this and related gestalt images.

is postulated to underly the *cognitive coordination* required for gestalt perception. Neural coordination is thought to be mediated by ensemble formation by matching of firing through oscillations in gamma and beta bands (Dumenko, 2002; Fries et al., 2007; Lisman and Idiart, 1995; Uhlhaas et al., 2006a). Therefore, schizophrenia illustrates a disorder where one can start to make connections between neural and cognitive processing; between the dynamics of oscillations, the flow of information, attribution of meaning, and coordination of perception.

**Technical aside – measuring nTE:** We used normalized transfer entropy (nTE) to measure the influence of synaptic inputs on spiking outputs, providing our information theoretic measure of information flow-through. The nTE algorithm allows us to determine how much signal, coming in as postsynaptic potentials (PSPs), comes out of the cell as a lagged spike output. A single cell with a Poisson input and identical lagged output (incoming EPSP reliably triggers a spike), provides full input/output information transfer – a loss-less communication line. In this case, nTE would be high, although it would not be 1.0 due both to the statistical nature of the measure and of its normalization. By contrast, two identical Poisson spike trains with no lag would have nTE near 0 – previous input does not predict output at all – predictability due to spike-train regularity will be subtracted out by the algorithm. When a cell is embedded within a network, in the present case within the CA3 network, the network itself interacts with the infor-

mation that flows from external inputs (local afferents) through the network to outputs (local efferents). We measured information flow cell-by-cell from external inputs (the drive) onto an individual pyramidal cell, with output the spiking of that cell. We then average these to get total *network nTE* (Fig. 10). This results in low nTE values that are nonetheless significant, as can be shown by assessing the change in nTE while gradually connecting up a network, starting from independent individual cells with no effect on one another (see Neymotin et al., 2011a, Fig. 76.10). The equation for transfer entropy is

$$TE_{X1\to X2} = H\left(X2_{\text{future}}|X2_{\text{past}}\right) - H\left(X2_{\text{future}}|X2_{\text{past}}, X1_{\text{past}}\right)$$

(Jumarie, 1990; Paluš, 1996; Hlaváckova-Schindler et al., 2007; Neymotin et al., 2011a); and for normalized transfer entropy:

$$nTE_{X1\to X2} = \frac{TE_{X1\to X2} - < TE_{X1_{\text{shuffled}}\to X2} >}{H(X2_{\text{future}}|X2_{\text{past}})}$$

(Gourevitch and Eggermont, 2007), where the mutual information $H$ is given by

$$H(X_{\text{future}}|X_{\text{past}}) = -\sum p(X_{\text{future}}, X_{\text{past}}) \log \frac{p(X_{\text{future}}, X_{\text{past}})}{p(X_{\text{past}})}$$

**Effect of NMDAR conductance on information flow-through**

Reduced OLM NMDAR conductance is associated not only with higher gamma but also with reduced information flow-through (Fig. 10). A correlation between dynamics and information capacity here is not unexpected: increased gamma is evidence of a dynamical structure that partially constrains spiking in the network – individual cell spike firing will occur with higher probability at the peak of the gamma cycle. This increased dynamical constraint is necessarily associated with a reduction in the ability of firing to follow inputs that come in at arbitrary times, a decrease in the number of possible states of the network, a decrease in network entropy. Borrowing a clinical term from schizophrenia, we can characterize this reduced entropy as *increased stereotypy*. This suggests that a reduction in variability of information flow, and information processing, in the gamma-bound network would be associated with a rigidity

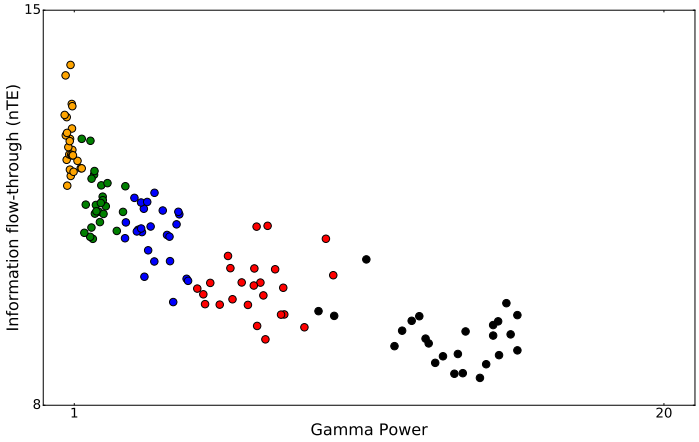


Figure 10: Shift in gamma power (x-axis) and information flow through the network as a function of OLM NMDAR conduction from orange (high, wild type) to lower values in sequence: green, blue, red, black. As gamma increases information flow-through measured by nTE decreases.

of thought and reduction of behavioral responsivity to changing circumstances. The thought patterns and behavior of patients suffering from schizophrenia do show this combination of reduced gestalt perceptual ability, decreased flexibility of thought (*e.g.,* in paranoia), and stereotypic patterns of behavior.

## The future

While only including a bare sketch of the scales circled in Fig. 11, our basic multiscale model of CA3 was used to provide connections from the molecular scale of genomics, proteomics and pharmacology to observations at the high levels of cognition and behavior. This is a "bare sketch" insofar as much detail has been omitted, even at the scales of focus – notably in the use of 5-compartment models for the pyramidal cells, leaving out the complexity of ion channel distribution across the dendritic tree and the complexities of dendritic signaling. This particular simplification can be explained by the limitations of knowledge and the limitations of computer power. Considering HCN, there is evidence for a difference in density at different locations in the pyramidal dendritic tree, possibly associated with differential distribution of HCN1 and HCN2 – however the details of this distribution are not fully described. With regard to computational load, the use of random background inputs and random specific wiring based on wiring densities between populations requires that we run multiple simulations to confirm the robustness and consistency of any

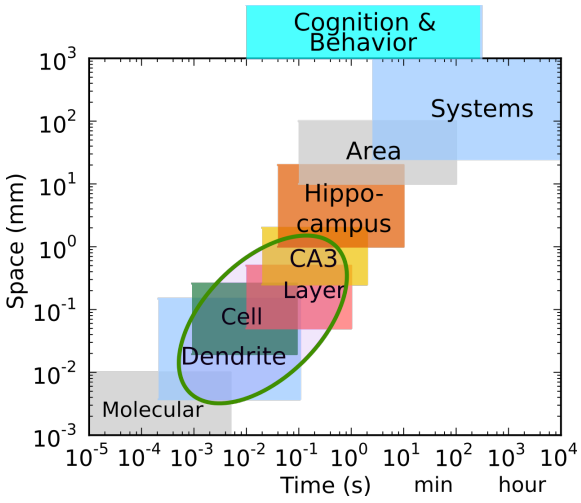


Figure 11: Scales for multiscale modeling. We have focused on the scale from dendrite to local circuit (green circle) but have reached downward to the level of molecules (synaptic receptor and ion channel populations) and upward to the levels of information and cognition. One key aspect of the multiscale brain is the great overlap across levels. An example is the wiring complexity (network scale) of projections from dentate gyrus and entorhinal cortex which show layer scale organization which directly impacts dendritic and cell processing due to the projection of dendrite across layers.

result, therefore requiring that even these relatively simple simulations be run on high performance computing (HPC) platforms (Lytton et al., in press).

Despite these many limitations, we are able to elaborate and extend existing general concepts that connect channel alterations to cell and network physiology, and connect network physiology to cognitive disorders of schizophrenia, allowing us to make specific predictions that would not be possible without representing each scale with needed detail. Rather than considering the minimum detail that is needed to represent the overall phenomenon, we ask what details are needed at each scale in order to be able to represent system queries (clinical tests) or system inputs (pharmacological, electrical, behavioral treatments) at these many scales.

We predict that the HCN and GRIN2 mutations suggested for schizophrenia are involved in the same clinical pathway, and that the abnormalities in this clinical pathway produce alterations in oscillations and in deficits in cognitive coordination. We specifically suggest that the GRIN2A-associated mutations associated with schizophrenia would produce *decreased* conductance for NMDARs on oriens-lacunosum-moleculare (OLM) cells, and that HCN1 mutations would involved *increased* conductance for $I_{\mathrm{h}}$ on basket

(BAS) cells and possibly on pyramidal cells as well. These alterations would be associated with augmented gamma activity in CA3 and reduced nTE from mossy fibers input to Schaffer collateral output.

Future simulations will tie CA3 together to other areas of hippocampus and then tie hippocampus together with frontal lobes, another location with prominent pathology in schizophrenia.

Along with consciousness, the holy grails of neuroscience include understanding how original thought occurs, and how memory is stored. Thought presumably emerges from the vast networks of interconnected networks of the brain. Deep learning using artificial neural network algorithms has captured some aspects of this complexity, but much remains to be learned. Phenomenologically, the breakdown of thought in thought in schizophrenia will offer clues both as to how thought functions in the brain, and how to connect that functioning to the underlying neuronal substrate. It is intriguing that the breakdown modes in schizophrenia go in to directions: 1. excessive looseness of thought where ideas are not well connected to other ideas (looseness of associations, disorganized schizophrenia); 2. excessive "tightness" of thought where many unrelated observations are bound together to create an aberrant, but coherent, world view (paranoid schizophrenia). Exploration of looseness versus tightness will bring a new dimension to the *binding problem* that will further our understanding of the process of thought.

## References


Accili E, Proenza C, Baruscotti M, DiFrancesco D (2002) From funny current to HCN channels: 20 years of excitation. *Physiology* 17:32–37.

Aponte Y, Lien C, Reisinger E, Jonas P (2006) Hyperpolarization-activated cation channels in fast-spiking interneurons of rat hippocampus. *J Physiol* 574:229–243.

Bender R, Brewster A, Santoro B, Ludwig A, Hofmann F, Biel M, Baram T et al. (2001) Differential and age-dependent expression of hyperpolarization-activated, cyclic nucleotide-gated cation channel isoforms 1-4 suggests evolving roles in the developing rat hippocampus. *Neuroscience* 106:689–698.

Börgers C, Kopell N (2003) Synchronization in networks of excitatory and inhibitory neurons with sparse, random connectivity. *Neural Comput* 15:509–538.

Bressler SL, Kelso J (2001) Cortical coordination dynamics and cognition. *Trends in cognitive sciences* 5:26–36.

Brody CD (1999) Correlations without synchrony. *Neural computation* 11:1537–1551.

Buzsáki G, Wang X (2012) Mechanisms of gamma oscillations. *Annu Rev Neurosci* 35:203–225.

Chen S, Wang J, Siegelbaum S (2001) Properties of hyperpolarization-activated pacemaker current defined by coassembly of HCN1 and HCN2 subunits and basal modulation by cyclic nucleotide. *Journal Gen Physiol* 117:491–504.

Chover J, Haberly L, Lytton W (2001) Alternating dominance of NMDA and AMPA for learning and recall: a computer model. *Neuroreport* 12:2503–2507.

Cobb S, Buhl E, Halasy K, Paulsen O, Somogyi P (1995) Synchronization of neuronal activity in hippocampus by individual GABAergic interneurons. *Nature* 378:75–78.

Cull-Candy S, Brickley S, Farrant M (2001) NMDA receptor subunits: diversity, development and disease. *Current Opinion in Neurobiology* 11:327 – 335.

Cutsuridis V, Graham B, Cobb S, Vida I (2010) *Hippocampal microcircuits: a computational modeler's resource book*, Vol. 5 Springer Science & Business Media.

de Haan W, van der Flier W, Wang H, Van Mieghem P, Scheltens P, Stam C (2012) Disruption of functional brain networks in alzheimer's disease: what can we learn from graph spectral analysis of resting-state magnetoencephalography? *Brain Connect* 2:45–55.

Dumenko V (2002) Functional significance of high-frequency components of brain electrical activity in the processes of gestalt formation. *Zh Vyssh Nerv Deiat Im I P Pavlova* 52:539–550.

Dyhrfjeld-Johnsen J, Morgan R, Földy C, Soltesz I (2008) Upregulated H-Current in hyperexcitable CA1 dendrites after febrile seizures. *Front Cell Neurosci* 2.

Dyhrfjeld-Johnsen J, Morgan R, Soltesz I (2009) Double trouble? potential for hyperexcitability following both channelopathic up-and downregulation of Ih in epilepsy. *Front Neurosci* 3:25.

Franck N, Duboc C, Sundby C, Amado I, Wykes T, Demily C, Launay C, Le Roy V, Bloch P, Willard D et al. (2013) Specific vs general cognitive remediation for executive functioning in schizophrenia: a multicenter randomized trial. *Schizophrenia research* 147:68–74.

Fries P, Nikolic D, Singer W (2007) The gamma cycle. *Trends Neurosci* 30:309–316.

Gourevitch B, Eggermont J (2007) Evaluating Information Transfer Between Auditory Cortical Neurons. *Journal of Neurophysiology* 97:2533.

Hagiwara N, Irisawa H (1989) Modulation by intracellular Ca2+ of the hyperpolarization-activated inward current in rabbit single sino-atrial node cells. *J Physiol* 409:121–141.

Hangya B, Borhegyi Z, Szilagyi N, Freund T, Varga V (2009) GABAergic neurons of the medial septum lead the hippocampal network during theta activity. *J Neurosci* 29:8094–8102.

Hasselmo M (2005) Expecting the unexpected: modeling of neuromodulation. *Neuron* 46:526–528.

Hasselmo M, Bower J (1992) Cholinergic suppression specific to intrinsic not afferent fiber synapses in rat piriform (olfactory) cortex. *J Neurophysiol* 67:1222–1229.

Hirano Y, Oribe N, Kanba S, Onitsuka T, Nestor P, Spencer K (2015) Spontaneous gamma activity in schizophrenia. *JAMA Psychiatry* 72:813–821.

Hlavácková-Schindler K, Palus M, Vejmelka M, Bhattacharya J (2007) Causality detection based on information-theoretic approaches in time series analysis. *Physics Reports* 441:1–46.

Insel T, Cuthbert B, Garvey M, Heinssen R, Pine DS, Quinn K, Sanislow C, Wang P (2010) Research domain criteria (rdoc): toward a new classification framework for research on mental disorders. *American Journal of Psychiatry* .

International Schizophrenia Consortium *et al.* (2009) Common polygenic variation contributes to risk of schizophrenia and bipolar disorder. *Nature* 460:748–752.

Jahr C, Stevens C (1990b) Voltage dependence of NMDA-activated macroscopic conductances predicted by single-channel kinetics. *J Neurosci* 10:3178–3182.

Jumarie G (1990) *Relative Information: Theories and Applications* Springer-Verlag New York, Inc. New York, NY, USA.

Lazarewicz M, Ehrlichman R, Maxwell C, Gandal M, Finkel L, Siegel S (2010) Ketamine modulates theta and gamma oscillations. *J Cogn Neurosci* 22:1452–1464.

Lee H, Dvorak D, Fenton A (2014) Targeting neural synchrony deficits is sufficient to improve cognition in a schizophrenia-related neurodevelopmental model. *Front Psychiatry* 5:15.

Lewis DA, Curley AA, Glausier JR, Volk DW (2012) Cortical parvalbumin interneurons and cognitive dysfunction in schizophrenia. *Trends Neurosci* 35:57–67.

Lisman J, Raghavachari S (2006) A unified model of the presynaptic and postsynaptic changes during ltp at ca1 synapses. *Science Signaling* .

Lisman J, Idiart M (1995) Storage of 7 ± 2 Short-Term Memories in Oscillatory Subcycles. *Science* 267:1512–1515.

Lytton W (2008) Computer modelling of epilepsy. *Nat Rev Neurosci* 9:626–637.

Lytton W, Seidenstein A, Dura-Bernal S, McDougal R, Schürmann F, Hines M (in press) Simulation neurotechnologies for advancing brain research: Parallelizing large networks in neuron. *Neural Computation* .

Lytton W, Sejnowski T (1991a) Simulations of cortical pyramidal neurons synchronized by inhibitory interneurons. *J Neurophysiol* 66:1059–1079.

Lytton W, Sejnowski T (1991b) Simulations of cortical pyramidal neurons synchronized by inhibitory interneurons. *J Neurophysiol* 66:1059–1079.

Moretti D, Paternicò D, Binetti G, Zanetti O, Frisoni G (2013) EEG upper/low alpha frequency power ratio relates to temporo-parietal brain atrophy and memory performances in mild cognitive impairment. *Front Aging Neurosci* 5:63.

Neymotin S, Hilscher M, Moulin T, Skolnick Y, Lazarewicz M, Lytton W (2013) Ih tunes theta/gamma oscillations and cross-frequency coupling in an in silico CA3 model. *PLoS One* 8:e76285.

Neymotin S, Jacobs K, Fenton A, Lytton W (2011a) Synaptic information transfer in computer models of neocortical columns. *J Comput Neurosci* 30:69–84.

Neymotin S, Lazarewicz M, Sherif M, Contreras D, Finkel L, Lytton W (2011b) Ketamine disrupts theta modulation of gamma in a computer model of hippocampus. *J Neurosci* 31:11733–11743.

Neymotin S, McDougal R, Bulanova A, Zeki M, Lakatos P, Terman D, Hines M, WW L (2016) Calcium regulation of HCN channels supports persistent activity in a multiscale model of neocortex. *Neurosci* 316:344–366.

Paluš M (1996) Detecting nonlinearity in multivariate time series. *Phys. Lett. A* 213:138–147.

Poolos NP, Bullis JB, Roth MK (2006) Modulation of h-channels in hippocampal pyramidal neurons by p38 mitogen-activated protein kinase. *J Neurosci* 26:7995–8003.

Poolos N, Migliore M, Johnston D (2002) Pharmacological upregulation of h-channels reduces the excitability of pyramidal neuron dendrites. *Nat Neurosci* 5:767–774.

Santoro B, Baram T (2003) The multiple personalities of h-channels. *Trends Neurosci* 26:550–554.

Schizophrenia Working Group (2014) Biological insights from 108 schizophrenia-associated genetic loci. *Nature* 511:421–427.

Sekar A, Bialas A, Rivera H, Davis A, Hammond T, Kamitaki N, Tooley K, Presumey J, Baum Me (2016) Schizophrenia risk from complex variation of complement component 4. *Nature* 530:177–183.

Serulle Y, Zhang S, Ninan I, Puzzo D, McCarthy M, Khatri L, Arancio O, Ziff EB (2007) A glur1-cgkii interaction regulates ampa receptor trafficking. *Neuron* 56:670–688.

Shannon CE, Weaver W (1949) *The Mathematical Theory of Communication* U Illinois Press.

Silverstein S, Hatashita-Wong M, Schenkel L, Wilkniss S, Kovács I, Fehér A, Smith T, Goicochea C, Uhlhaas P, Carpiniello K, Savitz A (2006) Reduced top-down influences in contour detection in schizophrenia. *Cogn Neuropsychiatry* 11:112–132.

Stacey W, Lazarewicz M, Litt B (2009) Synaptic noise and physiological coupling generate high-frequency oscillations in a hippocampal computational model. *J Neurophysiol* 102:2342–2357.

Stewart M, Fox S (1990) Do septal neurons pace the hippocampal theta rhythm. *Trends Neurosci* 13:163–168.

Sullivan P (2012) Puzzling over schizophrenia: schizophrenia as a pathway disease. *Nat Med* 18:210–211.

Tandon R, Gaebel W, Barch DM, Bustillo J, Gur RE, Heckers S, Malaspina D, Owen MJ, Schultz S, Tsuang M et al. (2013) Definition and description of schizophrenia in the DSM-5. *Schizophrenia research* 150:3–10.

Tort A, Rotstein H, Dugladze T, Gloveli T, Kopell N (2007) On the formation of gamma-coherent cell assemblies by oriens lacunosum-moleculare interneurons in the hippocampus. *Proc Nat Acad Sci* 104:13490–13495.

Tost H, Meyer-Lindenberg A (2012) Puzzling over schizophrenia: schizophrenia, social environment and the brain. *Nat Med* 18:211–213.

Traub R (1982) Simulation of intrinsic bursting in CA3 hippocampal neurons. *Neurosci* 7:1233–1242.

Uhlhaas P, Haenschel C, Nikolić D, Singer W (2008) The role of oscillations and synchrony in cortical networks and their putative relevance for the pathophysiology of schizophrenia. *Schizophrenia Bulletin* 34:927–943.

Uhlhaas P, Linden D, Singer W, Haenschel C, Lindner M, Maurer K, Rodriguez E (2006a) Dysfunctional long-range coordination of neural activity during gestalt perception in schizophrenia. *J Neurosci* 26:8168–8175.

Uhlhaas P, Phillips W, Mitchell G, Silverstein S (2006b) Perceptual grouping in disorganized schizophrenia. *Psychiatry Res* 145:105–117.

Uhlhaas P, Phillips W, Schenkel L, Silverstein S (2006c) Theory of mind and perceptual context-processing in schizophrenia. *Cognit Neuropsychiatry* 11:416–436.

Uhlhaas P, Silverstein S (2005) Perceptual organization in schizophrenia spectrum disorders: empirical research and theoretical implications. *Psychol Bull* 131:618–632.

Uhlhaas P, Singer W (2010) Abnormal neural oscillations and synchrony in schizophrenia. *Nature Rev Neurosci* 11:100–113.

Wahl-Schott C, Biel M (2009) HCN channels: structure, cellular regulation and physiological function. *Cel Mol Life Sci* 66:470–494.

Wang X (2002) Pacemaker neurons for the theta rhythm and their synchronization in the septohippocampal reciprocal loop. *J Neurophysiol* 87:889–900.

Wang X, Buzsaki G (1996) Gamma oscillation by synaptic inhibition in a hippocampal interneuronal network model. *J Neurosci* 16:6402–6413.

White J, Banks M, Pearce R, Kopell N (2000) Networks of interneurons with fast and slow $\gamma$-aminobutyric acid type A (GABAA) kinetics provide substrate for mixed gamma-theta rhythm. *Proc Nat Acad Sci* 97:8128–8133.

Zemankovics R, Káli S, Paulsen O, Freund T, Hájos N (2010) Differences in subthreshold resonance of hippocampal pyramidal cells and interneurons: the role of h-current and passive membrane characteristics. *J Physiol* 588:2109–2132.

Zong X, Krause S, Chen C, Krüger J, Gruner C, Cao-Ehlker X, Fenske S, Wahl-Schott C, Biel M (2012) Regulation of hyperpolarization-activated cyclic nucleotide-gated (HCN) channel activity by cCMP. *J Biol Chem* 287:26506–26512.